Journal of Statistical Physics, Vol. 53, Nos. 1/2, 1988

Stochastic Disk Dynamo as a Model of Reversals of the Earth's Magnetic Field

H. M. Ito[1]

Received April 13, 1988

A stochastic model is given of a system composed of N similar disk dynamos interacting with one another. The time evolution of the system is governed by a master equation of the class introduced by van Kampen as relevant to stochastic macrosystems. In the model, reversals of the earth's magnetic field are regarded as large deviations caused by a small random force of $O(N^{-1/2})$ from one of the field polarities to the other. Reversal processes are studied by simulation, which shows that the model explains well the activities of the palaeomagnetic field inclusive of statistical laws of the reversal sequence and the intensity distribution. Comparisons are made between the model and dynamical disk dynamo models.

KEY WORDS: Stochastic; disk dynamo; master equation; large deviation; reversal; earth's magnetic field.

1. INTRODUCTION

It is believed that the earth's magnetic field originates in a dynamo action in the core, a generation of a self-sustaining magnetic field through the interaction of the mechanical motion of a fluid and the flow of an electric current in the fluid.[1-3] One of the most intriguing theoretical problems in geophysics is how the dynamo action gives rise to reversals of the earth's field, which have occurred for the past 600 million years or much more.

In view of the intractability of the problem of the magnetohydrodynamic dynamo, an attempt is made to model the geomagnetic reversals. Theories of the dynamo suggest that fluid motion in the core is in turbulence and forms a number of eddies, which play a main role in the

[1] Seismology and Volcanology Division, Meteorological Research Institute, Tsukuba, Ibaraki 305, Japan.

0022-4715/88/1000-0019$06.00/0

dynamo action. If we assume that the eddies are approximated well by disk dynamos with a few degrees of freedom, a stochastic system of interacting disk dynamos will give a good picture of the dynamo action in the core. As long as the eddies are so located that the effects of their spatial distribution can be neglected, being coupled together through a mean-field-like interaction, and as long as the time evolution is Markovian, the system will be described by a class of master equations first introduced by van Kampen[4] in a study of stochastic processes of macrosystems.

He considers a macro-Markovian process $\Xi(t)$ proportional to the size of a macrosystem, and assumes that the transition rate $W(\mathbf{X}, \mathbf{r})$ of Ξ from $\mathbf{X}$ to $\mathbf{X}+\mathbf{r}$ has the form

$$W(\mathbf{X}, \mathbf{r}) = w(\varepsilon \mathbf{X}, \mathbf{r})/\varepsilon \tag{1.1}$$

with a certain function w, where ε is a small parameter denoting the inverse of the size of the system. Then the normalized process $\xi(t) = \varepsilon \Xi(t)$ is governed by a master equation of the form

$$\partial p(t, \mathbf{x})/\partial t = (1/\varepsilon) \int d\mathbf{r} \, \{w(\mathbf{x} - \varepsilon \mathbf{r}, \mathbf{r}) \, p(t, \mathbf{x} - \varepsilon \mathbf{r}) - w(\mathbf{x}, \mathbf{r}) \, p(t, \mathbf{x})\} \tag{1.2}$$

for a transition probability density $p(t, \mathbf{x})$ $[= P(\xi(t) \in d\mathbf{x})/d\mathbf{x}]$. $\xi(t)$ is regarded as a motion such that the dynamical motion

$$\dot{\mathbf{x}}(t) = \phi(\mathbf{x}(t)) \tag{1.3}$$

with

$$\phi(\mathbf{x}) = \int \mathbf{r} w(\mathbf{x}, \mathbf{r}) \, d\mathbf{r} \tag{1.4}$$

is perturbed by a small jump-type random force of order of $\varepsilon^{1/2}$ (see Appendix A). Van Kampen's model together with an approximation scheme in the limit of $\varepsilon \to 0$ has been developed by Kubo *et al.*[5] and Suzuki[6] and has been applied to many systems.[7]

As we will see in Section 3, if we take a single disk dynamo with viscous coupling as the model of an eddy, the limit equation (1.3) has two stable equilibrium points corresponding to the two polarities of the earth's magnetic field. The small random force is harmless for a short time interval, but eventually gives rise to large deviations from one of the equilibrium points to a neighborhood of the other, i.e., reversals of the earth's field. We will see that this view explains well the palaeomagnetic data. Another view has been proposed which regards the apparently irregular reversal sequence as "chaos" in dynamical systems, such as Rikitake's model.[8–10] Here we can make an interesting comparison between the two views.

Phenomena of large deviations, for example, relaxations from metastable states, have been studied by many authors (see refs. 11 and references therein; see also refs. 12), who have focused their attention mainly on the asymptotics of transition probability functions, eigenvalues of generators, means and variances of the first hitting times, and so on. One of the main concerns in the present paper, on the other hand, is how the flip-flop process on the polarities is derived, which is closely related to recent work on asymptotic distributions of occurrence times of rare events (see refs. 13 and 14; for mathematical monographs see refs. 15). While only a special example is discussed here, it is hoped that a new area for statistical physics is being opened up, one not entirely encompassed by the setups of refs. 13 and 14.

I begin with a review of observational and theoretical aspects of the reversal process of the earth's magnetic field in Section 2, which is supplemented by Appendix B, giving some details of the dynamical disk dynamo models. Section 3 is devoted to the construction of the model and discussion of its properties via simulation. Concluding remarks follow in Section 4.

2. OBSERVATIONAL AND THEORETICAL ASPECTS OF THE REVERSAL PROCESS

2.1. Evidence from Palaeomagnetic Studies

General information can be found in the monographs by Rikitate[1] and Merrill and McElhinny[3] or the review by Jacobs,[2] to which I mainly refer in the following to avoid citation of much literature. For further details see the references therein.

The earth's field has existed for at least 3000 million years and its strength has not significantly differed from its present value. For at least the past 600 million years it has been, on the average, approximated well by a geocentric dipole whose axis agrees with the earth's rotation axis. Reversals between the two polarities, conventionally called the normal polarity and the reverse polarity, have occurred at irregular times since the Precambrian, more than 600 million years ago. The length of polarity intervals, time intervals between two successive reversals, varies from 0.02 million years, the minimum detectable length, to several tens of millions of years. Reversals are completed in 10^3–10^4 years, and during transitions the field, after a considerable decrease in intensity, is dominated by the nondipole components. Phenomena called excursions, reminiscent of aborted reversals, have also been observed. The frequency of reversals averaged over the period 10–50 million years fluctuates widely with the

change of geological eras, which gives rise to the phenomenon of polarity bias.

More quantitative information is available for recent periods on temporal variations (ref. 16; ref. 3, Section 5.3) and intensity distribution (ref. 17; ref. 3, Section 6.3):

P1. The number $N(t)$ of reversals up to time t in the past 80 million years is well described by a Poisson process. A mild nonstationarity is observed; the intensity function $\lambda(t) = E[N(t)]$ has the form $\lambda_0 + \lambda_1 t$ where λ_1 increases at a rate of 0.05 per million years. In the past 10 million years stationarity may be assumed and $\lambda_1 \simeq 5 \times 10^{-6}$/year. No difference of statistical significance is observed between two sequences obtained by choosing either the normal or the reverse polarity.

Oscillations of the magnetic field with a period of 8000–9000 years and a striking discontinuity of $\lambda(t)$ around 45 million years ago quoted in ref. 2 are now regarded as highly tentative (ref. 16; ref. 3, Section 4.1.3).

P2. The density function f of the intensity of the dipole moment for the past 5 million years almost satisfies a symmetry of the two polarities suggested by that of the magnetohydrodynamic equation. Taking the dipole moment y to be positive or negative according as the polarity is normal or reverse, the following form, expressed as a sum of two truncated Gaussian distributions, is compatible with palaeomagnetic data:

$$f(y) = N_1 I_{(-\infty, -y_1]}\, g(y + y_0; \sigma_0) + N_2 I_{[y_2, \infty)}\, g(y - y_0; \sigma_0) \qquad (2.1)$$

where g is the Gaussian distribution

$$g(y; \sigma) = (2\pi\sigma^2)^{-1/2} \exp(-y^2/2\sigma^2) \qquad (2.2)$$

and I_A is the indicator function of the set A [$I_A(y) = 1$ if $y \in A$ and $= 0$ if $y \notin A$]. The normalization constants N_1, N_2 are chosen so that the integrals of f on positive and negative half-lines become 1/2. The parameters y_0 and σ_0 are estimated to be $8.67 \pm 0.65 \times 10^{22}$ A m^2 and $3.63 \pm 0.75 \times 10^{22}$ A m^2 with 95% confidence, respectively. The cutoff points y_1, y_2 appear because samples in transient periods are omitted in the statistical analysis. Only those samples are taken into account that have the associated virtual geomagnetic pole[2] with latitude greater than 45°. Under the assumption that $y_1 = y_2$, their maximum likelihood estimates are 2.75×10^{22} A m^2, about 30% of y_0.

[2] When the geomagnetic field is observed at one point on the surface of the earth, we can imagine a geocentric dipole which would produce the observed field at the point. The fictitious dipole is called the virtual dipole moment, and the intersection of its axis and the surface of the earth determines the virtual geomagnetic pole.

A closer examination of the data reveals a disagreement between y_1 and y_2 (the maximum likelihood estimates are 1.84×10^{22} and 3.11×10^{22} A m^2, respectively), suggesting a slight asymmetry between the two polarities. The nondipole components give a contribution proportional to $y\eta$, the product of the dipole moment y and a standard normal random variable η, to the virtual dipole moment. The proportionality constant is estimated at about 0.2.

When we refer to the properties P1 and P2 in the following, we consider the period of the past several million years unless otherwise stated: (P1) the number of reversals $N(t)$ is a stationary Poisson process, and (P2) the density function f of the dipole intensity has a symmetric double Gaussian distribution (2.1).

2.2. Reversal Models Based on Dynamo Theories

A full account of the above properties P1 and P2 based on magnetohydrodynamics is still beyond our reach, although the presence of reversals has been demonstrated numerically under some additional assumptions.[18] Studies on the dynamo action of systems with a few degrees of freedom, initiated by Bullard,[19,20] assume one or a few disk dynamos consisting of rotators, brushes, coils, etc. Each disk dynamo may represent an eddy in the earth's core, but it will be unnecessary to imagine counterparts of such accessories as the brushes or the coils, because ordinary differential equations governing the systems can be derived from the magnetohydrodynamic equations by truncation,[21] just as in the Lorenz system.[22]

The single disk dynamo due to Bullard[19,20] does not give rise to reversals. But the coupled two-disk dynamos due to Rikitake[8] as well as the shunted single-disk dynamo with an impedance between the brush and the coil due to Malkus[23] and Robbins[24] exhibit chaotic reversals.[8-10,23,24] A great nonuniformity in the frequency of reversals averaged over 10 million years, reminiscent of those of the earth's field, is observed in these two models.[24,25] However, there are qualitative differences between the properties of the models and the observed facts; the earth's field does not show growing oscillations preceding a reversal, contrary to the prediction by the models (see Fig. 1). Moreover, as stated in Section 2.1, the oscillations of the field are now regarded as highly tentative, and no great nonuniformity has been observed for the past 80 million years. Numerical calculations in Appendix B tell us that the above properties P1 and P2 are unlikely to be satisfied at the same time by the dynamical disk dynamo models.

There are many attempts based on theories of stochastic processes. An

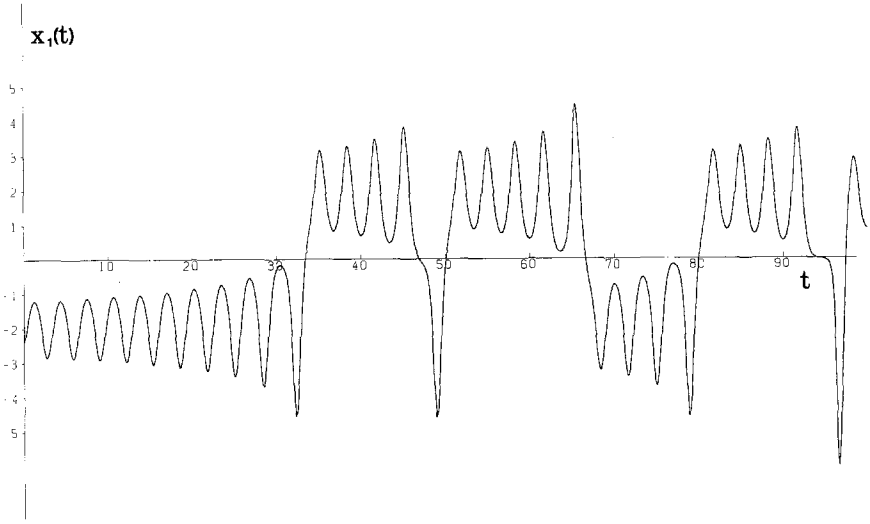

Fig. 1. Time plot of $x_1(t)$ of the Rikitake model (B.1) for $\mu = 1$, $K = 2$.

introduction is omitted here of the descriptions in terms of combinations of the dipole and the nondipole fields expressed by simple stochastic processes (ref. 2; ref. 3, Section 9.2), because they will be of little interest from a statistical mechanical point of view, though useful in practical situations. Parker[26] and Levy[27] have proposed the idea that reversals occur when the eddies in the earth's core, through random processes, arrive at a certain critical configuration. The property P1 suggests that a sequence of critical and noncritical configurations assumes a strong independence, forming, for example, a sequence of Bernoulli trials.[28] Unfortunately no justification has been given to the independence except for the case where the eddies move independently. Kono[29] has suggested that the dipole–dipole interaction between the eddies is a clue to understanding the reversal phenomena; the properties P1 and P2 are shared by a system of several interacting dipoles, similar to the kinetic Ising model with mean field interaction.[30] His idea will be developed in the present paper by introducing a dynamo action which sustains the dipole fields of the eddies.

3. STOCHASTIC DISK DYNAMO MODEL

3.1. Model Master Equation

Let us consider a system composed of N similar disk dynamos interacting with one another. As illustrated in Fig. 2, each disk rotates

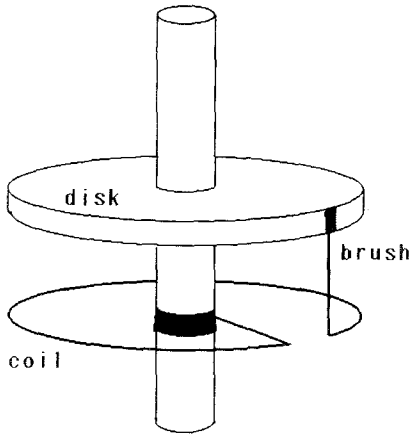

Fig. 2. Schematic diagram of single disk dynamo due to Bullard.[19]

about its axis in a field parallel to the axis, and current drawn from two brushes, one on the periphery and one on the axle of the disk, passes through a coil to produce the magnetic field. We may describe the system using two macrovariables, the total magnetic field produced by the currents and the total angular momentum of the disks. They can be substituted for an algebraic sum Ξ_1 of the currents in the coils and an algebraic sum Ξ_2 of the angular velocities as long as the disks are assumed to be so located that the effects of their spatial distribution can be neglected and their axes are parallel to one another. We put $\Xi = (\Xi_1, \Xi_2)$, and by $\xi = (\xi_1, \xi_2)$ we denote a vector normalized by N: $\xi = \Xi/N$.

We next determine the transition rate $W(\mathbf{X}, \mathbf{r})$ of (1.1). As stated in Section 1, ξ converges in the limit of $N \to \infty$ to certain $\mathbf{x} = (x_1, x_2)$ governed by a deterministic equation, which, we suppose, agrees with

$$L\dot{x}_1 = -Rx_1 + Mx_1x_2, \qquad C\dot{x}_2 = -kx_2 + G - Mx_1^2 \tag{3.1}$$

for a single disk dynamo with a viscous coupling term kx_2.[9] Here L is the self-inductance and R the resistance of the circuit, M is the mutual inductance between the coil and the disk, C is the moment of inertia of the disk, and G is the couple driving it. For notational convenience we introduce dimensionless variables ξ_1', ξ_2', x_1', x_2', and t' defined by

$$\begin{aligned} x_1' &= (M/G)^{1/2} x_1, \qquad x_2' = (MC/GL)^{1/2} x_2, \qquad t' = (GM/CL)^{1/2} t \\ \xi_1' &= (M/G)^{1/2} \xi_1, \qquad \xi_2' = (MC/GL)^{1/2} \xi_2, \end{aligned} \tag{3.2}$$

and then drop the prime on ξ_1', ξ_2', x_1', x_2', and t'. Then (3.1) becomes

$$\dot{x}_1 = -\mu x_1 + x_1 x_2, \qquad \dot{x}_2 = -\nu x_2 + 1 - x_1^2 \tag{3.3}$$

where the dimensionless parameters μ and ν are given by

$$\mu = (CR^2/GML)^{1/2}, \qquad \nu = (Lk^2/GCM)^{1/2} \tag{3.4}$$

The limit equation (3.3) is written as

$$\dot{X}_1 = -\mu X_1 + N^{-1} X_1 X_2, \qquad \dot{X}_2 = -\nu X_2 + N^{-1}(N^2 - X_1^2) \tag{3.5}$$

if we use an extensive variable $\mathbf{X} \equiv (X_1, X_2) = N\mathbf{x}$. In the stochastic model, to the term $-\mu X_1$ in the rhs of the first equation of (3.5), for example, there will correspond a rate $W_1(\mathbf{X}, \mathbf{r})$ which has a peak at $\mathbf{r} = (-\operatorname{sgn}(X_1), 0)$ and amounts to $\mu |X_1|$ when integrated over all $\mathbf{r}$. Assuming, for simplicity, a Gaussian form for W_1, we can write

$$W_1(\mathbf{X}, \mathbf{r}) = \mu |X_1| \, g(r_1 + \operatorname{sgn}(X_1); \sigma_1) \, g(r_2; \sigma_2)$$

with suitable parameters σ_1, σ_2. Here $\operatorname{sgn}(X_1)$ denotes the sign of X_1, and the Gaussian function g is defined by (2.2). By a similar discussion for the other three terms in the rhs of (3.5), we have

$$\begin{aligned} W(\mathbf{X}, \mathbf{r}) = {} & \mu |X_1| \, g(r_1 + \operatorname{sgn}(X_1); \sigma_1) \, g(r_2; \sigma_2) \\ & + \nu |X_2| \, g(r_1; \sigma_1) \, g(r_2 + \operatorname{sgn}(X_2); \sigma_2) \\ & + N^{-1} |X_1 X_2| \, g(r_1 - \operatorname{sgn}(X_1 X_2); \sigma_1) \, g(r_2; \sigma_2) \\ & + N^{-1} |N^2 - X_1^2| \, g(r_1; \sigma_1) \, g(r_2 - \operatorname{sgn}(N^2 - X_1^2); \sigma_2) \end{aligned} \tag{3.6}$$

This kernel W clearly has the property (1.1) with

$$\begin{aligned} w(\mathbf{x}, \mathbf{r}) = {} & \mu |x_1| \, g(r_1 + \operatorname{sgn}(x_1); \sigma_1) \, g(r_2; \sigma_2) \\ & + \nu |x_2| \, g(r_1; \sigma_1) \, g(r_2 + \operatorname{sgn}(x_2); \sigma_2) \\ & + |x_1 x_2| \, g(r_1 - \operatorname{sgn}(x_1 x_2); \sigma_1) \, g(r_2; \sigma_2) \\ & + |1 - x_1^2| \, g(r_1; \sigma_1) \, g(r_2 - \operatorname{sgn}(1 - x_1^2); \sigma_2) \end{aligned} \tag{3.7}$$

and $\varepsilon = 1/N$. It is easy to check that the limit equation (1.3) with (1.4) agrees with (3.3). Thus we have obtained our model given by the master equation (1.2) with (3.7).

We have to infer the asymptotic behavior of ξ as $N \to \infty$ by simulations with relatively small N ($\leqslant 15$), mainly due to the restriction of computational time. Big jumps occurring frequently for small N ($\leqslant 3$)

make it difficult to obtain statistically stable results, hence concealing the dependence on N. So in the following we will simulate not only the jump model ξ, but also a diffusion model ζ given by a stochastic differential equation

$$\begin{aligned} d\zeta_1(t) &= [-\mu\zeta_1(t) + \zeta_1(t)\,\zeta_2(t)]\,dt + \varepsilon^{1/2}\,dw_1(t) \\ d\zeta_2(t) &= [-\nu\zeta_2(t) + 1 - \zeta_1(t)^2]\,dt + \varepsilon^{1/2}\,dw_2(t) \end{aligned} \tag{3.8}$$

with a small random force. Here $(w_1(t), w_2(t))$ is a two-dimensional Brownian motion, and $\varepsilon = 1/N$.

3.2. Method of Simulation

When $\mu\nu < 1$, which we shall study below, (3.3) has three equilibrium points, $S(0, \nu^{-1})$, $F_+(\lambda, \mu)$, and $F_-(-\lambda, \mu)$, where $\lambda = (1-\mu\nu)^{1/2}$. The point S is a saddle point, and F_+ and F_- are stable points with characteristic roots

$$s = -\nu/2 \pm (\nu^2 - 8\lambda^2)^{1/2}/2 \tag{3.9}$$

As $t \to \infty$, $(x_1(t), x_2(t))$ approaches F_+, F_-, or S according as $x_1(0) > 0$, $x_1(0) < 0$, or $x_1(0) = 0$.[9,31]

As will be seen later by simulation, the density function of the sojourn time of the current ξ_1 has peaks around $x_1 = \pm\lambda$ for large N, and $x_1 = \pm 0.3\lambda$ indicate, in view of the property P2 in Section 2.1, the boundaries of the two polarities. Hence we may divide the phase $x_1 - x_2$ plane into three regions as illustrated in Fig. 3: the reverse polarity $x_1 \leqslant -0.3\lambda$, the transient region $-0.3\lambda < x_1 < 0.3\lambda$, and the normal polarity $x_1 \geqslant 0.3\lambda$. To fix ideas, ξ is supposed to be initially in the reverse polarity. ξ will go into the normal polarity and back to the reverse polarity and so on. Corresponding to this sequence we define the first hitting times $\{\tau_i\}$ of the two polarities as follows:

$$\begin{aligned} \tau_0 &= 0 \\ \tau_{2n-1} &= \inf\{t > \tau_{2n-2};\, \xi_1(t) \geqslant 0.3\lambda\} \\ \tau_{2n} &= \inf\{t > \tau_{2n-1};\, \xi_1(t) \leqslant -0.3\lambda\}, \qquad n \geqslant 1 \end{aligned} \tag{3.10}$$

The polarity intervals of the normal and the reverse polarities are defined by $\{\tau_{2n} - \tau_{2n-1}\}$ and $\{\tau_{2n+1} - \tau_{2n}\}$ $(n \geqslant 1)$, respectively.[3] Time intervals

[3] Instead of $\{\tau_k - \tau_{k-1}\}$ it would be better to use $\{\tau'_k - \tau_{k-1}\}$ with τ'_k in (3.11). But the differences $\{\tau_k - \tau'_k\}$ are negligible compared with $\{\tau_k - \tau_{k-1}\}$ in the statistical sense.

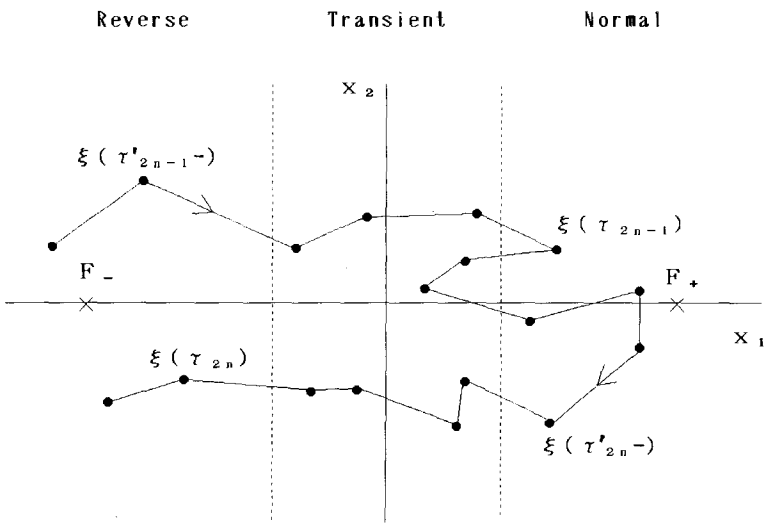

Fig. 3. Schematic division of the x_1–x_2 plane: the reverse polarity $x_1 \leqslant -0.3\lambda$, the transient region $-0.3\lambda < x_1 < 0.3\lambda$, and the normal polarity $0.3\lambda \leqslant x_1$. The polygonal line represents a sample path of ξ, and τ_n, τ'_n are the first hitting time and the last exit time of the polarities defined by (3.10), (3.11). $F_{\pm}$ are two stable equilibrium points of (3.3).

spent during transitions are given by $\{\tau_n - \tau'_n\}$ $(n \geqslant 1)$ where the τ'_n are the last exit times from the two polarities defined by

$$\begin{aligned} \tau'_{2n-1} &= \sup\{t < \tau_{2n-1};\, \xi_1(t) \leqslant -0.3\lambda\} \\ \tau'_{2n} &= \sup\{t < \tau_{2n};\, \xi_1(t) \geqslant 0.3\lambda\}, \qquad n \geqslant 1 \end{aligned} \tag{3.11}$$

During a short time interval Δt, ξ starting at $\mathbf{x}$ makes a transition to the $d(\varepsilon\mathbf{r})$ neighborhood of $\mathbf{x} + \varepsilon\mathbf{r}$ with probability $\varepsilon^{-1} w(\mathbf{x}, \mathbf{r})\, \Delta t\, d\mathbf{r}$, so that we can simulate the process ξ as follows. First we take mutually independent two-dimensional random variables α and β such that α assumes values $(-\mathrm{sgn}(x_1), 0)$, $(0, -\mathrm{sgn}(x_2))$, $(\mathrm{sgn}(x_1 x_2), 0)$, $(0, \mathrm{sgn}(1 - x_1^2))$, and $(0, 0)$ with corresponding probabilities

$$\begin{gathered} \mu\,|x_1|\,\Delta t/\varepsilon, \qquad \nu\,|x_2|\,\Delta t/\varepsilon \\ |x_1 x_2|\,\Delta t/\varepsilon, \qquad |1 - x_1^2|\,\Delta t/\varepsilon \\ 1 - \Delta t\{\mu\,|x_1| + \nu\,|x_2| + |x_1 x_2| + |1 - x_1^2|\}/\varepsilon \end{gathered}$$

and such that β is Gaussian having mean $(0, 0)$ and covariance matrix $(\sigma_i \delta_{ij})$. For a realized value $(\mathbf{a}, \mathbf{b})$ of (α, β), we move ξ by $(\mathbf{a} + \mathbf{b})\varepsilon$ if $\mathbf{a} \neq (0, 0)$, and put the clock forward by Δt. The method for the simulation of the diffusion model ζ of (3.8) will be obvious.

3.3. Results of Simulation

To simplify the discussion, we fix the parameters μ, σ_1, and σ_2 to be 0.3 throughout this subsection because the model seems to depend on these parameters less sensitively than on v.

The step functions $h_N(t)$ in Fig. 4 [(a) $N=5$, $v=0.5$, (b) $N=15$, $v=0.5$] give approximate density functions of normalized polarity interval t, obtained from the frequency distributions of polarity intervals in simulated reversal sequences. In both cases $h_N(t)$ fits with the exponential function e^{-t}, suggesting that the reversal sequences are Poissonian. This point has been examined more quantitatively by using another test of goodness of fit for Poisson processes[32]: if a reversal sequence is observed for a fixed time interval $[0, T_0]$ and n reversals occur at T_1, T_2,..., T_n in $(0, T_0)$, then T_i/T_0 $(i=1, 2,..., n)$ are independently and uniformly distributed over $(0, 1)$, which is checked by the two-sided Kolmogorov–Smirnov test. In each case of N, 10 sample sequences were generated, and the Poisson hypothesis was always retained at the 5% level of significance, except for one sequence with $N=15$. The $h_N(t)$ with $N=5$ in Fig. 4a has a dip for $t \lesssim 0.2$, which always happened for the other nine sample sequences. On the other hand, no systematic deviation from the exponential function was observed for $N=15$. These facts will allow us to assume a better fit to

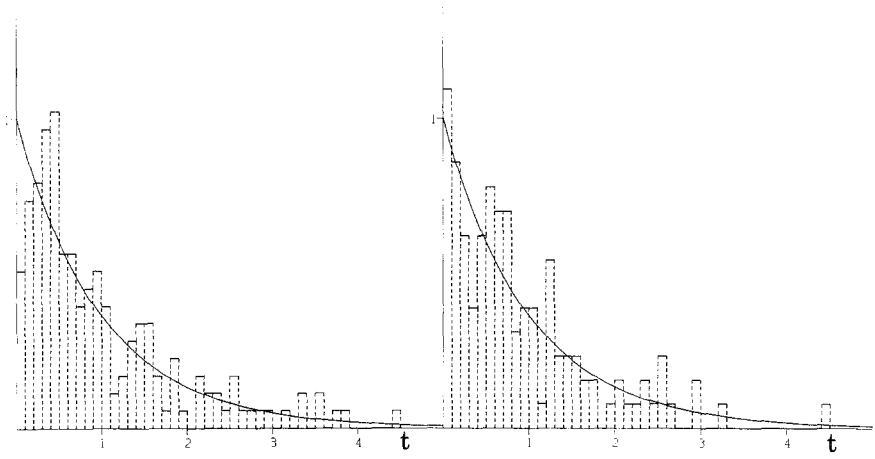

Fig. 4. Step function h_N giving approximate density functions of polarity intervals for (a) $\mu=0.3$, $v=0.5$, $\sigma_1=\sigma_2=0.3$, $N=5$, and (b) $\mu=0.3$, $v=0.5$, $\sigma_1=\sigma_2=0.3$, $N=15$. The h_N are obtained as follows: for $t \in [i/10, (i+1)/10)$, $i=0, 1, 2,...$, $h_N(t)=10$ multiplied by the relative frequency of polarity intervals in $[mi/10, m(i+1)/10)$, where m is the sample mean giving a unit of time axis. The decreasing function in the figure is the exponential function e^{-t}. The numbers of polarity intervals used for the analyses are (a) 176 and (b) 128.

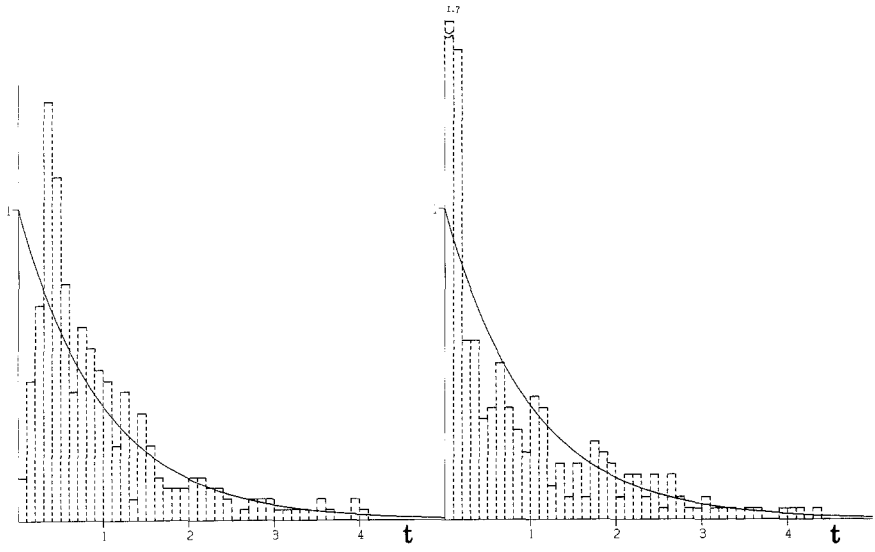

Fig. 5. As in Fig. 4, but for (a) $\mu = 0.3$, $\nu = 0.1$, $\sigma_1 = \sigma_2 = 0.3$, $N = 5$, and (b) $\mu = 0.3$, $\nu = 0.1$, $\sigma_1 = \sigma_2 = 0.3$, $N = 20$. The numbers of polarity intervals used for the analyses are (a) 290 and (b) 278.

Poisson processes for larger N. This point can be checked more quantitatively in the diffusion model (see below).

The asymptotic behavior for $N \to \infty$ depends, however, on the parameter ν. When ν is changed from 0.5 to 0.1, the intensity of $h_N(t)$ for smaller t ($\leqslant 0.2$) grows as N increases, and finally exceeds substantially the expected value of the exponential function (Fig. 5).

This phenomenon may be interpreted in terms of the following property of the dynamical equation (3.3) actually governing ξ for large N. The characteristic roots (3.9) indicate that the attractive forces of the points $F_\pm$ are weak for small ν, implying a frequent appearance of ξ located near the polarity boundaries $(\pm 0.3\lambda, x_2)$ with a large, negative x_2. By the first equation of (3.3), we see that the x_2 axis attracts such ξ strongly, giving rise to reversals with relatively short polarity intervals. This interpretation is supported by the observation that the percentage of reversals occurring on the negative half-plane $x_2 < 0$ increases from about 20% to almost 100% as ν decreases from 0.5 (Fig. 4b) to 0.1 (Fig. 5b).

The density function of the sojourn time of $\xi_1(t)$ depends on ν and N in a rather simple way; the double Gaussian distribution (2.1) gives a good approximation for large N and ν (Fig. 6). The density function of the time $\tau_n - \tau'_n$ spent during reversals is unimodal and its rise becomes sharper as ν or N increases (Fig. 7).

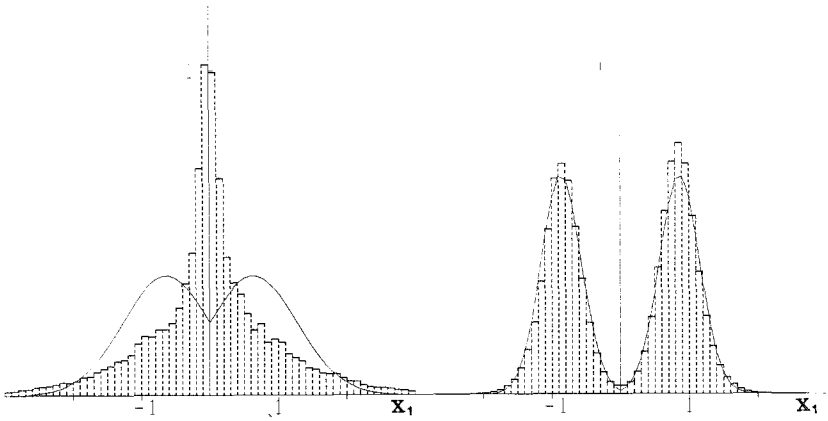

Fig. 6. Step function f_N giving the approximate density functions of the sojourn time of $\xi_1(t)$ for (a) $\mu=0.3$, $\nu=0.1$, $\sigma_1=\sigma_2=0.3$, $N=5$, and (b) $\mu=0.3$, $\nu=0.5$, $\sigma_1=\sigma_2=0.3$, $N=15$. The $f_N(x)$ are obtained as follows: for $x\in[i/10, (i+1)/10)$, $i=0, \pm1, \pm2,\ldots$, $f_N(x)=10$ multiplied by the proportion of the sojourn time of ξ_1 on $[i/10, (i+1)/10)$. The bimodal functions are given by (2.1) where y_0 and σ_0 are the sample mean and standard deviation of the sojourn time of $|\xi_1(t)|$.

The diffusion model ζ is qualitatively the same as ξ in the asymptotics of the above-discussed three quantities. The convergence of reversal sequences as $N\to\infty$ to Poisson processes when $\mu=0.3$, $\nu=0.5$ can be checked more clearly than in the case of ξ. Of 10 sample sequences with $N=1$ the Poisson hypothesis was rejected with a 5% level of significance

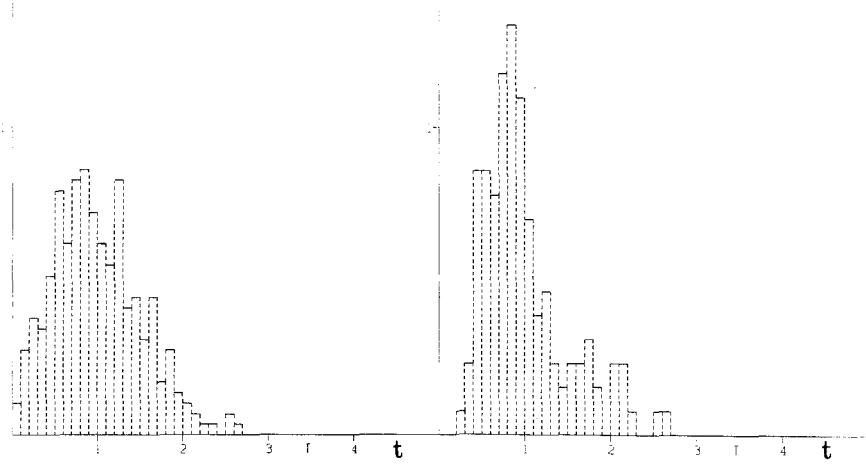

Fig. 7. Step functions giving approximate density functions of time spent during transitions $\{\tau_n-\tau'_n\}$ for (a) $\mu=0.3$, $\nu=0.1$, $\sigma_1=\sigma_2=0.3$, $N=5$, and (b) $\mu=0.3$, $\nu=0.5$, $\sigma_1=\sigma_2=0.3$, $N=15$. The step functions are constructed in the same manner as h_N in Fig. 4.

by two samples and with a 10% level by one sample. On the other hand, the hypothesis was always retained with a 10% level of significance by 10 sample sequences with $N = 15$.

3.4. Comparison with the Observed Facts

First we give estimated values of geophysical parameters. In Eq. (3.1), L/R represents the free decay time of the magnetic field, being of the order of 10^4 years (ref. 3, Section 7.4.3), so that the unit of time $\mu L/R$ becomes of the order of $\mu \times 10^4$ years [see (3.2)]. Values of the parameter μ range from 10^{-3} to 10.[10] The decay time $(1/\nu)\,\mu(L/R)$ years of the disk may be equated with that of the velocity of the fluid in the core due to viscosity. Estimating the latter time scale by (radius of the core)^2/kinetic viscosity and using values 3×10^6 m for the radius and 10^{-6} to 10^5 m^2 sec^{-1} for the viscosity of the core (ref. 3, Section 7.1), we have $\mu/\nu = 3 \times 10^{-4}$ to 3×10^7. These restrictions on μ and ν have been fulfilled in Section 3.3.

For the cases with $\mu = 0.3$, $\nu = 0.5$, and $\sigma_1 = \sigma_2 = 0.3$ discussed in Section 3.2, values of $N = 10$–11 together with $L/R \simeq 5000$ years explain well the observed facts P1 and P2. The Poisson property of the reversal sequences as well as the double Gaussian form of the intensity distribution are satisfied. The average polarity length is about 0.2–0.3 million years. The parameters y_0 and σ_0 are 0.82–0.83 and 0.37–0.36, respectively; the ratio σ_0/y_0 agrees with the observed value 3.63/8.67. The average time spent during transitions is about 5×10^3 years, of order of the magnitude of the observed value 10^3–10^4 years.

Better choices of the parameters μ, ν, σ_1, σ_2, and N may be possible, but too small ν will not be adopted because it will violate, as we have seen in Section 3.3, the Poisson property of the reversal sequence. Our model in turn gives a restriction on the value of the viscosity of the core, which is known only vaguely.

The rest of the properties in Section 2.1 may be discussed in the present framework; the nonstationarity of reversal processes and the asymmetry between the two polarities may be interpreted by the time dependence of μ and ν and by statistical fluctuation, respectively. But I refrain from going into these too geophysical details.

4. CONCLUDING REMARKS

I have shown that the stochastic disk dynamo model written as (1.2) with (3.7) can explain well the observed facts P1 and P2 of Section 2.1. The contribution of this work, however, lies in the presentation of a general view of the reversal phenomena of the earth's field rather than in the

construction of the model or discussion of its physical contents. The present result together with that of Kono[29] suggests that the reversals can be considered as phenomena of large deviations in stochastic systems driven by small, random forces, physically in systems where 10–20 eddies in the earth's core evolve stochastically, coupled together through a mean-field-like interaction. This view gives a better account of the observed facts than the view which regards the reversal phenomena as "chaos" in dynamical disk dynamo models.

The present view should be reinforced and developed further. First we need to answer theoretically what kind of flip-flop process on the two polarities is expected asymptotically as $N \to \infty$. This can be done most directly by investigating the distribution of polarity intervals $\{\tau_k - \tau_{k-1}\}$ defined in Section 3, say

$$\lim_{K \to \infty} K^{-1} \sum_{k=1}^{K} I_A(\tau_k - \tau_{k-1})$$

Occurrences of rare events such as polarity reversals are expected to constitute Poisson processes. The simulation in Section 3 shows that the asymptotic Poisson property is not necessarily acquired, if, for example, ν is too small. In other words, the asymptotics of the flip-flop process seems to behave in a more complex way than anticipated from the asymptotic exponentiality of the first exit times from domains containing a stable point.[13] Second, we need to construct the model starting from assumptions on mutual interaction between the eddies, as is done for the kinetic Ising model[30] or the Maxwellian gas model.[33] The constructions not only give a vivid physical picture of the geodynamo, but also pave the way for a discussion of the stochastic behavior of the earth's dipole as a vector, which has been intensively studied recently.[34]

APPENDIX A. JUMP-TYPE STOCHASTIC DIFFERENTIAL EQUATION CORRESPONDING TO (1.2)

In d-dimensional jump-type stochastic differential equations, the role of a random force is played by a Poisson random measure ν characterized by the following properties [in this Appendix, ν is distinct from the parameter in (3.4)]: for disjoint subsets A_i $(i = 1, 2, \ldots)$ of $[0, \infty) \times R^d$, $\nu(A_i)$ are mutually independent Poisson random variables and satisfy the countable additivity $\nu(\bigcup_i A_i) = \sum_i \nu(A_i)$. We assume that the intensity function $E[\nu(dt \times d\mathbf{u})]$ has the form $dt \times d\mathbf{u}$. Let us consider a jump-type stochastic differential equation

$$d\xi(t) = \mathbf{b}(\xi(t)) + \varepsilon \int_{R^d} \mathbf{c}(\xi, \mathbf{u})\, \tilde{\nu}(\varepsilon^{-1}\, dt \times d\mathbf{u}) \tag{A.1}$$

for d-dimensional vector functions $\mathbf{b}$ and $\mathbf{c}$. Here $\tilde{v}(*) = v(*) - E[v(*)]$. If we put

$$w(\mathbf{x}, \mathbf{r}) = \int I_{d\mathbf{r}}(c(\mathbf{x}, \mathbf{u}))\, d\mathbf{u}/d\mathbf{r} \tag{A.2}$$

where I_A is the indicator of the set A, and if $\mathbf{b}$ is related to $\mathbf{c}$ as

$$\mathbf{b}(\mathbf{x}) = \int \mathbf{c}(\mathbf{x}, \mathbf{u})\, d\mathbf{u} \tag{A.3}$$

then the probability density function $P(\xi(t) \in d\mathbf{x})/d\mathbf{x}$ satisfies the master equation (1.2). The above fact can be proved by using Itô's formula for jump-type stochastic differential equations.[35,36]

The smallness of the second term on the rhs of (A.1) is certified from

$$E\left[\left|\varepsilon \int \mathbf{c}(\xi, u)\, \tilde{v}(\varepsilon^{-1}\, dt \times d\mathbf{u})\right|^2\right] = \varepsilon E\left[\int |\mathbf{c}(\xi, \mathbf{u})|^2\, dt\, d\mathbf{u}\right] = O(\varepsilon) \tag{A.4}$$

More precisely, $\xi(t)$ converges to $\mathbf{x}(t)$ of (1.3), and $\varepsilon^{-1/2}(\xi(t) - \mathbf{x}(t))$ does to a Gaussian process

$$d\eta(t) = \mathbf{B}(\mathbf{x}(t))\, \eta(t)\, dt + \mathbf{D}(\mathbf{x}(t))\, d\mathbf{w}(t) \tag{A.5}$$

with

$$B_{ij}(x) = \partial b_i(x)/\partial x_j \tag{A.6}$$

$$\sum_k D_{ik}(\mathbf{x})\, D_{jk}(\mathbf{x}) = \int c_i(\mathbf{x}, \mathbf{u})\, c_j(\mathbf{x}, \mathbf{u})\, d\mathbf{u} \tag{A.7}$$

which can be proved by using a convergence theorem of stochastic differential equations (ref. 36, p. 338, Theorem 3, and pp. 238, 273). I do not go into the details here. See also refs. 6 and 37 for other proofs of the above convergence theorem.

APPENDIX B. STATISTICAL PROPERTIES OF THE DYNAMICAL DISK DYNAMOS

We investigate whether the models by Rikitake[8] and by Malkus[23] and Robbins[24] satisfy the statistical properties P1 and P2 discussed in Section 2.1.

The Rikitake model consists of two similar disk dynamos coupled so that the current from each feeds the coil of the other (Fig. 8), and is determined by differential equations with a parameter μ,

$$\dot{x}_1 = -\mu x_1 + x_2 x_3, \qquad \dot{x}_2 = -\mu x_2 + x_4 x_1, \qquad \dot{x}_3 = \dot{x}_4 = 1 - x_1 x_2 \quad \text{(B.1)}$$

in a dimensionless form. Here x_1 and x_2 represent the currents of the two circuits, and x_3 and x_4 are the angular velocities of the two disks. The difference of the angular velocities $x_4 - x_3$ is a constant of motion, which we shall conveniently write $-\mu(K^2 - K^{-2})$, and (B.1) is reduced to a three-dimensional $x_1 x_2 x_3$ system with a variable parameter K. The reduced system has two unstable equilibrium points $(K, K^{-1}, \mu K^2)$ and $(-K, -K^{-1}, \mu K^2)$. A trajectory encircles one of the equilibrium points several times and switches rapidly to encircle the other, without being captured by either. The μ–K plane is divided into periodic and chaotic regimes according to the mode of the switching phenomena (see ref. 25 for a phase diagram). In the chaotic regime a narrow zone called the minimum entropy regime is observed where sequences show great nonuniformity in reversal frequency, mimicking well the geodynamo activity.[25] Estimates of geophysically plausible μ values range from 10^{-3} to 10, and the value of K adopted in previous studies[10,25] is of order unity. Of (μ, K) in the chaotic regime, we discuss the case (R1) $\mu = 1$, $K = 2$,[10] and, as an example lying very close to the minimum entropy regime, the case (R2) $\mu = 1.95$, $K = 3$. Figure 1 shows the behavior of $x_1(t)$, where growing oscillations result in reversals. From this figure polarity intervals may be defined by two successive zero crossing points of $x_1(t)$. As a unit of time we take $\mu \times 10^4$ years (see Section 3.4).

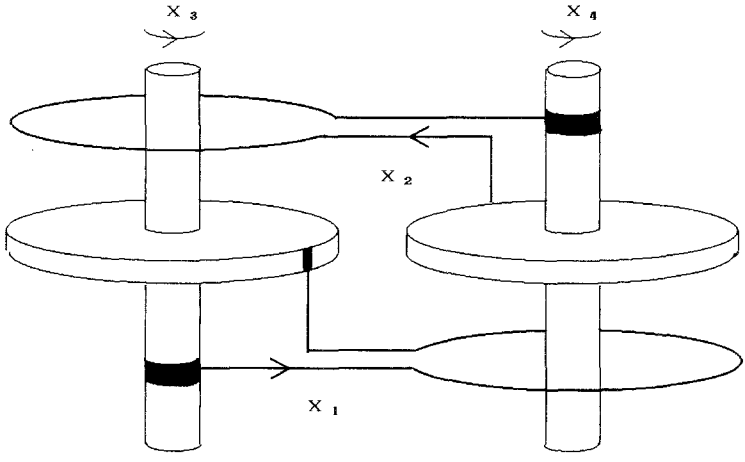

Fig. 8. Schematic diagram of the Rikitake model.

R1. A sequence is analyzed which spans about 10 million years and contains 176 reversals. The polarity intervals are nearly integral multiples of a mean period T_0 ($\simeq 0.03$ million years) of the oscillations. The root mean square of $T_i - T_0$ ($i = 1, 2, \ldots$) is less than about 1% of T_0, where T_i is the average period of oscillations in the ith polarity interval. Furthermore, the relative frequency of polarity intervals counted in units of T_0 approximately follows an exponential distribution with mean 0.1 million years (Fig. 9a). These two facts show that the reversal process is roughly a sequence of Bernoulli trials when viewed in units of T_0. If the effects of the spatial distribution of the two disk dynamos are neglected, the total magnetic field produced by the system is proportional to $x_1 + x_2$. Simulation of the density functions of its sojourn time (Fig. 10a), however, is not compatible with the double Gaussian distribution (2.1).

R2. A sequence is analyzed which spans about 70 million years and contains 139 reversals. The quantization of polarity intervals of mean period T_0 ($\simeq 0.04$ million years) of oscillations is still observed, but the density function of polarity intervals deviates substantially from the exponential function with mean 0.6 million years (Fig. 9b). The density function of the sojourn time of $x_1 + x_2$ has distinct maxima around K and/or $-K$. But it becomes hard to realize the equal weight of the two polarities (Fig. 10b) as a result of the nonuniformity in reversal frequency, especially for a shorter time span, say, several million years.

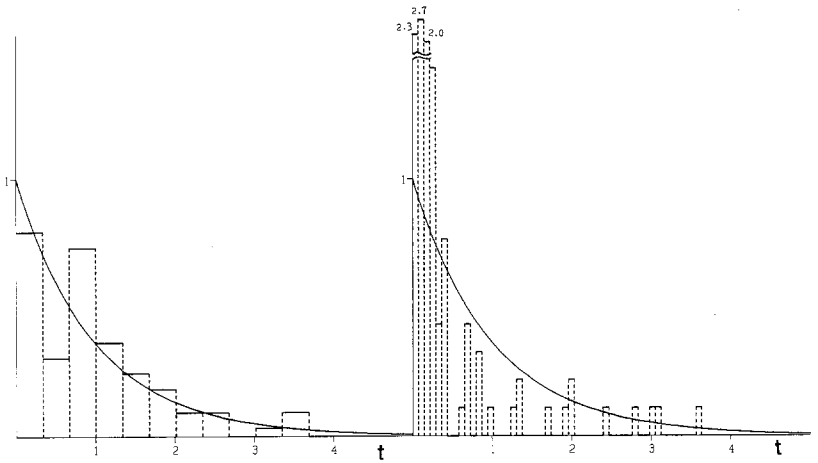

Fig. 9. Step functions giving approximate density functions of polarity intervals of the Rikitake model for (a) $\mu = 1$, $K = 2$ and (b) $\mu = 1.95$, $K = 3$. The step functions are constructed in the same manner as h_N in Fig. 4, but the step width is T_0, the mean cycle of oscillations. The time axis is normalized by the mean of polarity intervals. The numbers of polarity intervals used for the analyses are (a) 96 and (b) 114.

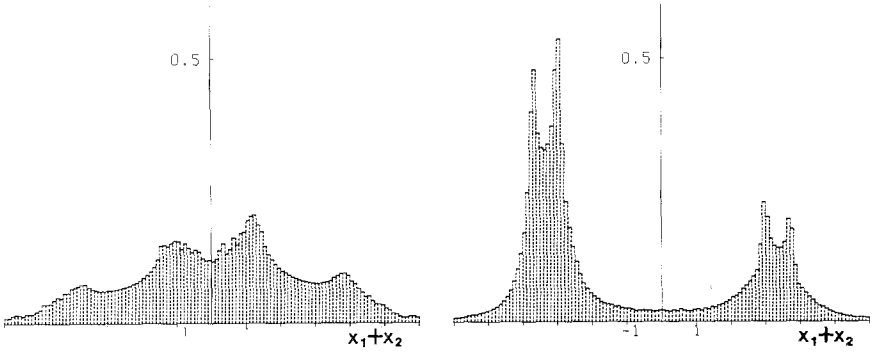

Fig. 10. Step functions giving approximate density functions of the sojourn time of $x_1(t)+x_2(t)$ of the Rikitake model for (a) $\mu=1$, $K=2$, (b) $\mu=1.95$, $K=3$.

The Malkus–Robbins model is obtained by adding a shunt across the external circuit to the single-disk dynamo and by assuming the resistance and inductance of the brush on the periphery of the disk (Fig. 11). We will treat the case that the shunt has no inductance, which Robbins has studied most extensively. The differential equation governing the model is written in a dimensionless form as

$$\dot{x}_1=\sigma(x_2-x_1), \qquad \dot{x}_2=x_3x_1-x_2, \qquad \dot{x}_3=G-x_1x_2-\nu x_3 \quad \text{(B.2)}$$

with three parameters σ, G, and ν. Here x_1 and x_2 are currents flowing in the circuit and the disks, respectively, the latter of which is responsible for the observable field (the poloidal field). The variable x_3 is the angular

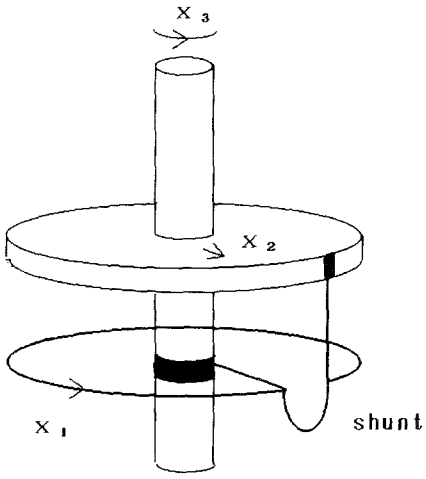

Fig. 11. Schematic diagram of the Malkus–Robbins model.

velocity of the disk. By a simple transformation $-x_1 \to x_1$, $-x_2 \to x_2$, $-x_3 + G/\nu \to x_3$, (B.2) is reduced to the canonical form of the Lorenz system.[22] For G just above $G_0 = \sigma\nu(\sigma + \nu + 3)/(\sigma - 1 - \nu)$ almost any trajectory exhibits chaotic reversals. There exists a subcritical region $G_1 < G < G_0$ where some of the trajectories tend asymptotically to the stable equilibrium points $(\pm(G-\nu)^{1/2}, \pm(G-\nu)^{1/2}, 1)$ of (B.2), while others tend to the so-called strange attractors, showing chaotic reversals indefinitely.[38] The number of oscillations between reversals fluctuates widely when G comes near G_1 from above, which leads Robbins to assert a corroboration of the model's relationship to the geodynamo.

We have taken $\sigma = 10$ and $\nu = 8/3$, giving $G_0 \simeq 65.97$ and $G_1 \simeq 64.16$, and examined the range of $64.11 \lesssim G \lesssim 74.67$. The quantization of polarity intervals in units of the oscillation period is observed. Our concern is the density function of polarity intervals measured in units of the period and that of the sojourn time of $x_1(t)$. The two functions are qualitatively similar to those shown in Figs. 9a and 10a except for a neighborhood $U(G_1)$ of G_1.[4] In $U(G_1)$ the characteristics of Figs. 9b and 10b are found, which we have confirmed only incompletely because the size of $U(G_1)$ is too small.

Our study suggests that the dynamical disk dynamo models due to Rikitake and Malkus and Robbins are unlikely to satisfy the properties P1 and P2 at the same time. It will be interesting to see whether the situation is improved by changing the values of the parameters or by using more complex dynamical disk dynamo models.[40] A success of a simple dynamical model of the solar dynamo[41] will give us a clue to a solution of the fundamental problem whether or not mechanisms of the dynamo action are different in the sun and in the earth.

[4] An exponential law for the polarity length in the Lorenz model was found by Aizawa.[39]

REFERENCES

1. T. Rikitake, *Electromagnetism and the Earth's Interior* (Elsevier, 1966).
2. J. A. Jacobs, *Phys. Rep. C* **26**:183 (1976).
3. R. T. Merrill and M. W. McElhinny, *The Earth's Magnetic Field* (Academic Press, 1983).
4. N. G. van Kampen, *Can. J. Phys.* **39**:551 (1961); in *Fluctuation Phenomena in Solids*, R. E. Burgess, ed. (Academic Press, 1965), Chapter 5.
5. R. Kubo, K. Matsuo, and K. Kitahara, *J. Stat. Phys.* **9**:51 (1973).
6. M. Suzuki, *Prog. Theor. Phys.* **53**:1657 (1975); **55**:383 (1976); *J. Stat. Phys.* **14**:129 (1976); **20**:163 (1979).
7. K. Tomita and H. Tomita, *Prog. Theor. Phys.* **51**:1731 (1974); K. Tomita, T. Ohta, and H. Tomita, *Prog. Theor. Phys.* **52**:1744 (1974); T. Takagahara, *Prog. Theor. Phys.* **53**:589 (1974); N. Ohata and M. Suzuki, *J. Phys. Soc. Jpn.* **39**:1175 (1975); H. Daido and K. Tomita, *Prog. Theor. Phys.* **61**:825 (1979).
8. T. Rikitake, *Proc. Camb. Phil. Soc.* **54**:89 (1958).

9. D. W. Allan, *Proc. Camb. Phil. Soc.* **58**:671 (1962).
10. A. E. Cook and P. H. Roberts, *Proc. Camb. Phil. Soc.* **68**:547 (1970).
11. G. H. Weiss, *J. Stat. Phys.* **42**:3 (1986); P. Hanggi, *J. Stat. Phys.* **42**:105 (1986).
12. Y. Saito, *J. Phys. Soc. Jpn.* **41**:388 (1976); K. Matsuo, K. Lindenberg, and K. E. Shuler, *J. Stat. Phys.* **19**:65 (1978); M. Moreau, *Physica* **90A**:410 (1978); B. Caroli, C. Caroli, and B. Roulet, *J. Stat. Phys.* **21**:415 (1979); **26**:83 (1981); W. Ebeling and L. Schimansky-Geier, *Physica* **98A**:587 (1979); B. Caroli, C. Caroli, B. Roulet, and J. F. G. Gouyet, *J. Stat. Phys.* **22**:515 (1980).
13. D. J. Aldous, *Stochastic Process Appl.* **13**:305 (1982); M. V. Day, *Stochastics* **8**:297 (1983); C. Kipnis and C. M. Newman, *SIAM J. Appl. Math.* **45**:972 (1982); M. Williams, *SIAM J. Appl. Math.* **42**:149 (1982).
14. M. Cassandro, A. Galves, E. Olivieri, and M. E. Vares, *J. Stat. Phys.* **35**:603 (1984); R. H. Schonmann, *J. Stat. Phys.* **41**:445 (1985); J. L. Lebowitz and R. H. Schonmann, *J. Stat. Phys.* **48**:727 (1987).
15. M. I. Freidlin and A. D. Wentzell, *Random Perturbations of Dynamical Systems* (Springer, 1984); S. R. S. Varadhan, *Large Deviations and Applications* (SIAM, 1984).
16. P. L. McFadden and R. T. Merril, *J. Geophys. Res.* **89**:3354 (1984).
17. P. L. McFadden and M. W. McElhinny, *J. Geomag. Geoelectr.* **34**:163 (1982).
18. D. Gubbins, *Geophys. J. R. Astron. Soc.* **42**:295 (1975); H. Watanabe, *J. Geomag. Geoelectr.* **33**:531 (1981).
19. E. C. Bullard, *Proc. Camb. Phil.* **51**:744 (1955).
20. E. Bullard, in *Topics in Nonlinear Dynamic*, S. Jorna, ed. (American Institute of Physics, 1978), p. 373.
21. P. Nozières, *Phys. Earth Planet. Interior* **17**:55 (1978).
22. E. N. Lorenz, *J. Atmos. Sci.* **20**:130 (1963).
23. W. V. R. Malkus, *EOS, Trans. Am. Geophys. Union* **53**:617 (1972).
24. K. A. Robbins, *Proc. Natl. Acad. Sci. USA* **73**:4297 (1976); *Math. Proc. Camb. Phil. Soc.* **82**:309 (1977).
25. K. Ito, *Earth Planet. Sci. Lett.* **51**:451 (1980).
26. E. N. Parker, *Astrophys. J.* **158**:815 (1969).
27. E. H. Levy, *Astrophys. J.* **171**:621, 635 (1972); **175**:573 (1972).
28. A. Cox, *J. Geophy. Res.* **75**:7501 (1970).
29. M. Kono, *Phys. Earth Planet. Interior* **5**:140 (1972).
30. R. B. Griffiths, C. Y. Weng, and J. S. Langer, *Phys. Rev.* **149**:301 (1966).
31. H. M. Ito, *J. Stat. Phys.* **35**:151 (1984).
32. D. R. Cox and P. A. W. Lewis, *The Statistical Analysis of Series of Events* (Methuen, 1966), Sections 6.2, 6.3.
33. M. Kac, In *Proceedings Third Berkeley Symposium on Mathematical Statistics and Probability*, Vol. III, p. 171 (1956); *Acta Phys. Austriaca* (Suppl.) **X**:379 (1973); H. P. Mckean, *Proc. Natl. Acad. Sci. USA* **56**:1907 (1966); *Commun. Pure Appl. Math.* **28**:435 (1975).
34. S. W. Bogue and K. A. Hoffmann, *Rev. Geophys.* **25**:910 (1987).
35. A. V. Skorohod, *Studies in the Theory of Random Processes* (Addison-Wesley, 1965).
36. I. I. Gihman and A. V. Skorohod, *Stochastic Differential Equations* (Springer, 1972).
37. T. G. Kurtz, *Approximation of Population Processes* (SIAM, 1981).
38. J. A. Yorke and E. D. Yorke, *J. Stat. Phys.* **21**:263 (1979); C. Sparrow, *The Lorenz Equations: Bifurcations, Chaos, and Strange Attractors* (Springer, 1982).
39. Y. Aizawa, *Prog. Theor. Phys.* **68**:64 (1982).
40. N. R. Lebovitz, *Proc. Camb. Phil. Soc.* **56**:154 (1969); T. Miura and T. Kai, *Phys. Lett.* **101A**:450 (1984).
41. N. O. Weiss, *J. Stat. Phys.* **39**:477 (1985).